The Journal of Neuroscience, January 1, 1997, 17(1):160–170

Low-Threshold Ca^{2+} Currents in Dendritic Recordings from Purkinje Cells in Rat Cerebellar Slice Cultures

Didier Mouginot, Jean-Louis Bossu, and Beat H. Gähwiler

Brain Research Institute, University of Zurich, CH-8029 Zurich, Switzerland

Voltage-dependent Ca^{2+} conductances were investigated in Purkinje cells in rat cerebellar slice cultures using the whole-cell and cell-attached configurations of the patch-clamp technique. In the presence of 0.5 mM Ca^{2+} in the extracellular solution, the inward current activated with a threshold of -55 ± 1.5 mV and reached a maximal amplitude of 2.3 ± 0.4 nA at -31 ± 2 mV. Decay kinetics revealed three distinct components: a fast (24.6 ± 2 msec time constant), a slow (304 ± 46 msec time constant), and a nondecaying component. Rundown of the slow and sustained components of the current, or application of antagonists for the P/Q-type Ca^{2+} channels, allowed isolation of the fast-inactivating Ca^{2+} current, which had a threshold for activation of -60 mV and reached a maximal amplitude of 0.7 nA at a membrane potential of -33 mV. Both activation and steady-state inactivation of this fast-inactivating Ca^{2+} current were described with Boltzmann equations, with half-activation and inactivation at -51 mV and -86 mV, respectively. This Ca^{2+} current was nifedipine-insensitive, but its amplitude was reduced reversibly by bath-application of $NiCl_2$ and amiloride, thus allowing its identification as a T-type Ca^{2+} current. Channels with a conductance of 7 pS giving rise to a fast T-type ensemble current (insensitive to ω-Aga-IVA) were localized with a high density on the dendritic membrane. Channel activity responsible for the ensemble current sensitive to ω-Aga-IVA was detected with 10 mM Ba^{2+} as the charge carrier. These channels were distributed with a high density on dendritic membranes and in rare cases were also seen in somatic membrane patches.

Key words: T-type calcium channels; cerebellum; Purkinje cells; patch clamp; dendritic recordings; cerebellar slice cultures

Voltage-activated Ca^{2+} channels in mammalian neurons have been shown to control many physiological processes, such as transmitter release, neuronal integration, and the generation of neuronal firing patterns. The existence of different types of voltage-activated Ca^{2+} channels accounts for the variety of these cellular functions (for review, see McCleskey, 1994), and six classes of Ca^{2+} channels (termed T, L, N, P, Q, and R) have been distinguished kinetically, pharmacologically, and molecularly (for review, see Bean, 1989; Tsien et al., 1991; Snutch and Reiner, 1992; McCleskey, 1994).

There is overwhelming physiological (Llinás et al., 1989; Usowicz et al., 1992) and molecular (Stea et al., 1995) evidence that Purkinje cells (PCs) express high levels of high-threshold P/Q-type Ca^{2+} channels. Whether functional T-type Ca^{2+} channels exist on cerebellar PCs remains controversial. Although some groups found no evidence for the presence of these channels in adult guinea pigs and young rats (Llinás and Sugimori, 1980a,b; Mintz et al., 1992a,b; Usowicz et al., 1992), others found T-type Ca^{2+} channels in PCs of young and adult rats (Bossu et al., 1989a,b; Hirano and Hagiwara, 1989; Kaneka et al., 1990; Regan, 1991). In the present study, we investigated both the presence and localization of Ca^{2+} channels in PCs by using cerebellar slice cultures and Ca^{2+} or Ba^{2+} as charge carriers.

Received July 12, 1996; revised Oct. 15, 1996; accepted Oct. 22, 1996.

This study was supported by the Human Frontier Science Program (Grant RG 67/92 B) and the Swiss National Science Foundation (Grant 31-42174.94). We thank L. Rietschin and L. Heeb for the preparation of slice cultures and E. Hochreutener and R. Schöb for technical assistance. We also thank Dr. N. A. Saccomano for the gift of ω-Aga-IVA and Drs. S. M. Thompson and Q. J. Pittman for critical reading and correction of this manuscript. Many thanks to J. C. Poncer and Dr. S. B. Kombian for their assistance with computer software.

Correspondence should be addressed to Dr. Didier Mouginot at Health Science Center, Neuroscience Research Group, Department of Medical Physiology, 3330 Hospital Drive NW, Calgary, Alberta, Canada T2N 4N1.

Jean-Louis Bossu's present address: Laboratoire de Neurobiologie Cellulaire, Centre National de la Recherche Scientifique, Centre de Neurochimie, 5 Rue Blaise Pascal, F-67084 Strasbourg Cedex, France.

Copyright © 1996 Society for Neuroscience 0270-6474/96/170160-11$05.00/0

MATERIALS AND METHODS

Preparation of cerebellar slice cultures

Organotypic cultures were prepared from cerebella removed from newborn rat pups (0–1 d old) and cultured as described previously (Gähwiler, 1981). In short, the cerebellum was dissected under aseptic conditions, and parasagittal slices of 400 μm thickness were cut with a McIlwain tissue chopper. Individual slices were embedded in clotted chicken plasma on glass coverslips and cultured by means of the roller tube technique at 36°C. The cultures were fed once a week with a medium consisting of 25% heat-inactivated horse serum, 50% Eagle's basal medium, and 25% HBSS, containing 33.3 mM D-glucose and 0.1 mM glutamine. Electrophysiological recordings were made after a period of >2 weeks *in vitro*.

Electrophysiology

Cerebellar slice cultures were transferred to a recording chamber mounted on the stage of an inverted microscope (Axiovert 35M, Zeiss, Jena, Germany), and all experiments were performed at room temperature (25°C). Patch-clamp recordings were carried out under voltage clamp in both the whole-cell recording (WCR) and cell-attached configurations, using an Axopatch 200A amplifier (Axon Instruments, Foster City, CA).

WCR configuration. For the WCR experiments, electrodes were pulled with a Flaming/Brown micropipette puller (Model P-87, Sutter Instruments, San Rafael, CA) using hematocrit glass tubes (plain microhematocrit tubes, no. 564; Assistent). Electrodes were filled with a solution containing (in mM): 3 $CaCl_2$, 2 $MgCl_2$, 20 tetraethylammonium chloride (TEACl), 100 HEPES, 30 EGTA (pCa^{2+} 10^{-8} M), 2 MgATP, and 0.5 GTP. The pH was adjusted to 7.2 with CsOH. Electrodes had a final tip resistance of 1.4 ± 0.15 MΩ. The extracellular solution had the following composition (in mM): 120 trichloroacetic acid (TCA), 0.5 or 1

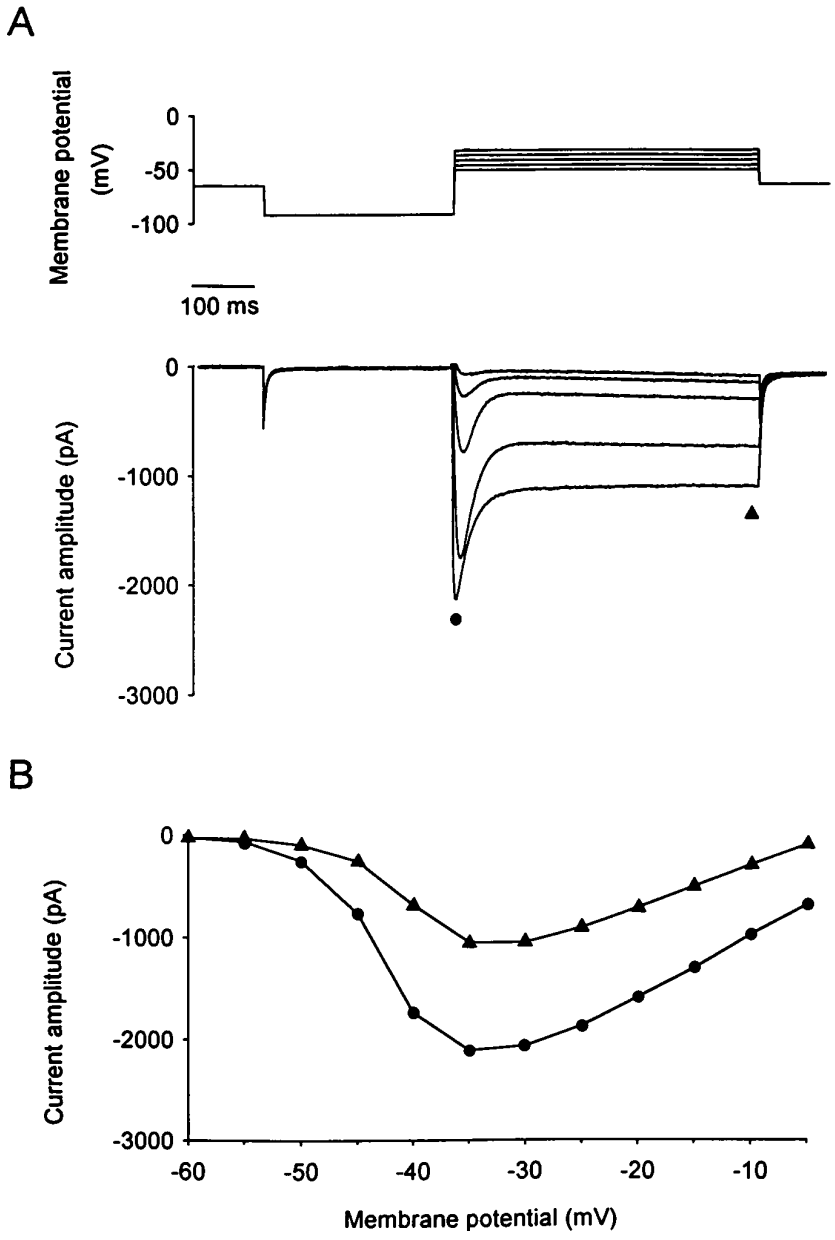

Figure 1. Macroscopic Ca^{2+} currents recorded from PCs in cerebellar slice cultures. *A*, Ca^{2+} current elicited in PCs with depolarizing voltage steps (500 msec) ranging from −55 to −35 mV in 5 mV increments. To remove inactivation of the Ca^{2+} current, a hyperpolarizing prepulse to −90 mV was applied before the voltage steps. *B*, Current–voltage relationship for the peak current (*filled circles*) and the sustained current measured at the end of the 500 msec depolarizing voltage steps (*filled triangles*) for the same cell as in *A*. Note that $[Ca^{2+}]_e$ of the saline was 0.5 mM.

$CaCl_2$, 3 $MgCl_2$, 20 TEACl, 10 HEPES/CsOH, phenol red (7%). TCA was substituted for NaCl to remove both Na^+- and Ca^{2+}-activated Cl^- currents (Bossu et al., 1991). The pH of the TCA stock solution (250 mM) and the extracellular solution were adjusted to 7.4 with Tris-base buffer (2.5 M).

PCs in organotypic cultures display an extensive dendritic arborization that could produce voltage-clamp artifacts. Therefore, recordings from PCs that had leak current exceeding 10 pA or recordings showing notable space-clamp artifacts were excluded from this study. The remaining cells had an average membrane capacitance of 61.6 ± 23 pF and a series resistance of 4 ± 2.5 MΩ (n = 20). Whole-cell and series-resistance compensation were applied.

Macroscopic Ca^{2+} currents were studied by using the software pClamp 5.5 (Axon Instruments) and digitized at 10 kHz (Digidata 1200A, Axon Instruments) before storage on a computer hard disk for off-line analysis (Clampfit 6, Axon Instruments).

Cell-attached configuration. For the experiments performed using the cell-attached configuration, the electrodes were pulled with a vertical puller (L/M-3P-A, List Medical, Darmstadt, Germany) using hematocrit glass tubing (Clark Electromedical Instruments, Reading, UK). To reduce the capacitance of the glass, the tip of the electrode was coated with a thick layer of a synthetic polymer (RTV 141, Rhône Poulenc, Lyon, France). Electrodes were filled with a solution containing (in mM): 120 TEACl, 10 $CaCl_2$, 2 $MgCl_2$, 1 CsCl, 10 HEPES, 1 4-aminopyridine. The pH was adjusted to 7.2 with a Tris-base solution (2.5 M). In some experiments $CaCl_2$ was replaced with $BaCl_2$, as indicated in the text and figure legends. The final tip resistance of the electrodes was 5–10 MΩ. The extracellular solution had the following composition (in mM): 137 NaCl, 2.7 KCl, 2.8 $CaCl_2$, 2 $MgCl_2$, 11.6 $NaHCO_3$, 0.4 NaH_2PO_4, 5.6 glucose. The pH was fixed at 7.4 by bubbling with 95% O_2/5% CO_2. Tetrodotoxin (5×10^{-7} M) was added to the bathing solution to block propagation of action potentials and to reduce release of neurotransmitter, which may change the resting potential (RP) of the recorded cell.

Voltage steps were elicited with a stimulus generator (Model PG 4000A, Neuro Data Instruments, Delaware Water Gap, PA), and the resulting current traces were filtered at 10 kHz and digitized at 47.2 kHz using a digital data recorder (VR-10B, Instrutech, Great Neck, NY) before storage on a video recorder (Panasonic NV-SD 30). For off-line analysis, data were sampled at 5 kHz and filtered with a cut-off frequency of 1.5 kHz (PClamp 6, Axon Instruments). Individual current traces were leak-subtracted before they were averaged. The leak subtraction was performed using averaged episodes that did not show channel openings. Numerical values are given as mean ± SEM.

Chemicals. ω-Conotoxin-MVIIC was purchased from Latoxan (Rosans,

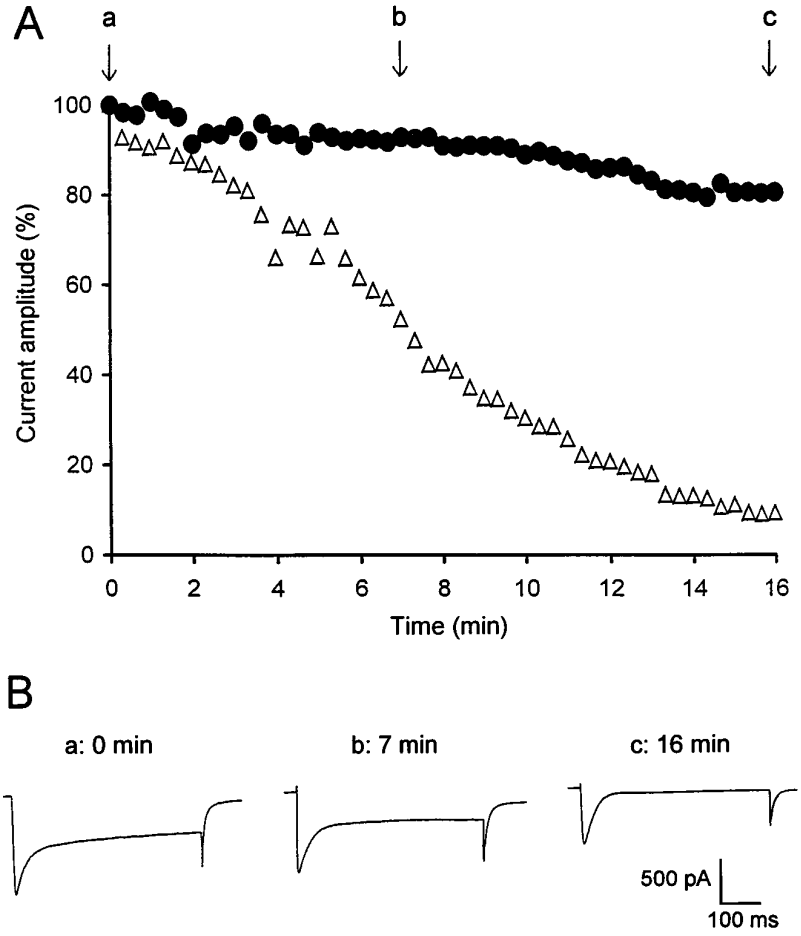

Figure 2. Isolation of a fast-inactivating Ca^{2+} current after rundown of both the slowly decaying and sustained components of the total Ca^{2+} current. *A*, Current amplitudes were determined every 20 sec. In the absence of ATP and GTP in the electrode solution, the amplitude of the sustained current (*open triangles*), measured at the end of the depolarizing voltage steps, markedly decreased with time, whereas the transient current (*filled circles*), defined as the difference between the peak and the sustained current, remained relatively stable. *B*, Examples of the total Ca^{2+} current measured just after disruption of the membrane-patch (*a*) and 7 (*b*) and 16 (*c*) min after establishment of the WCR.

France), and ω-Aga-IVA was a gift from Dr. N. A. Saccomano (Pfizer, Groton, CT). The two drugs were prepared as 100 μM stock solutions in distilled water and stored at −80°C. Before use, aliquots were diluted to 10 μM in extracellular solution containing 1 mg/ml cytochrome C (Sigma, St. Louis, MO). (−)β-Baclofen (β-*p*-chlorophenyl-GABA) was provided by Ciba Geigy (Basel, Switzerland). Amiloride and nifedipine were purchased from Sigma. All drugs were diluted to their final concentration just before bath application.

RESULTS

Somatic whole-cell and somatodendritic cell-attached recordings were performed from PCs in cerebellar slice cultures maintained for 15–31 d *in vitro*. Living PCs were identified by the size and shape of their soma and dendritic arborization and by their location within the culture (Gähwiler, 1981).

Characteristics of the macroscopic Ca^{2+} current

PCs were maintained at a holding potential of −70 mV. Hyperpolarizing voltage steps to −90 mV (300 msec) were first applied to remove possible steady-state inactivation of Ca^{2+} currents, followed by depolarizing voltage steps (500 msec) of increasing amplitude to elicit voltage-dependent Ca^{2+} currents (see voltage protocol in Fig. 1*A*). With an external Ca^{2+} concentration ($[Ca^{2+}]_e$) of 0.5 mM, depolarizing voltage steps elicited an inward current displaying complex decay kinetics, including both transient and sustained components (Fig. 1*A*). Kinetic analysis using a multi-exponential function was performed on the current at maximal amplitude ($n = 16$). This type of analysis revealed the presence of three distinct components for the decay: a fast (25 ± 2 msec time constant), a slow (304 ± 46 msec time constant detected in 64% of the cells analyzed), and a nondecaying or sustained component. To compare the voltage dependency for activation of transient and sustained current components, as well as their relative contribution to the total current, current–voltage relationships were obtained by measuring the amplitude of the current at its peak value (including the fast, slow, and sustained components), and at the end of the depolarizing voltage step (500 msec), to measure the sustained component alone (Fig. 1*B*). The peak current had a threshold for activation of −55 ± 1.5 mV, whereas the sustained component activated at a more depolarized potential (−43 ± 1 mV). Both components, however, reached a maximal amplitude at a similar membrane potential (−31 ± 2 mV and −29 ± 2 mV for the peak and the sustained current, respectively). The maximal peak current amplitude was −2.3 ± 0.4 nA, and the amplitude of the sustained current was −1.31 ± 0.3 nA.

The $[Ca^{2+}]_e$ was raised to 1 mM in the remaining experiments to increase the amplitude of the fast-inactivating Ca^{2+} current.

Isolation of the fast-inactivating Ca^{2+} current after rundown of both the slow and the sustained components

In the absence of ATP and GTP in the electrode solution, a decline of the Ca^{2+} current was observed once the WCR configuration had been established. The amplitude of the peak and the sustained currents were measured every 20 sec during this rundown process. The sustained current clearly decreased much faster (92.4 ± 3.2% reduction, measured after 17 min) than the peak current (51.5 ± 3.7% reduction). This procedure thus allowed the isolation of the fast-decaying transient current, defined

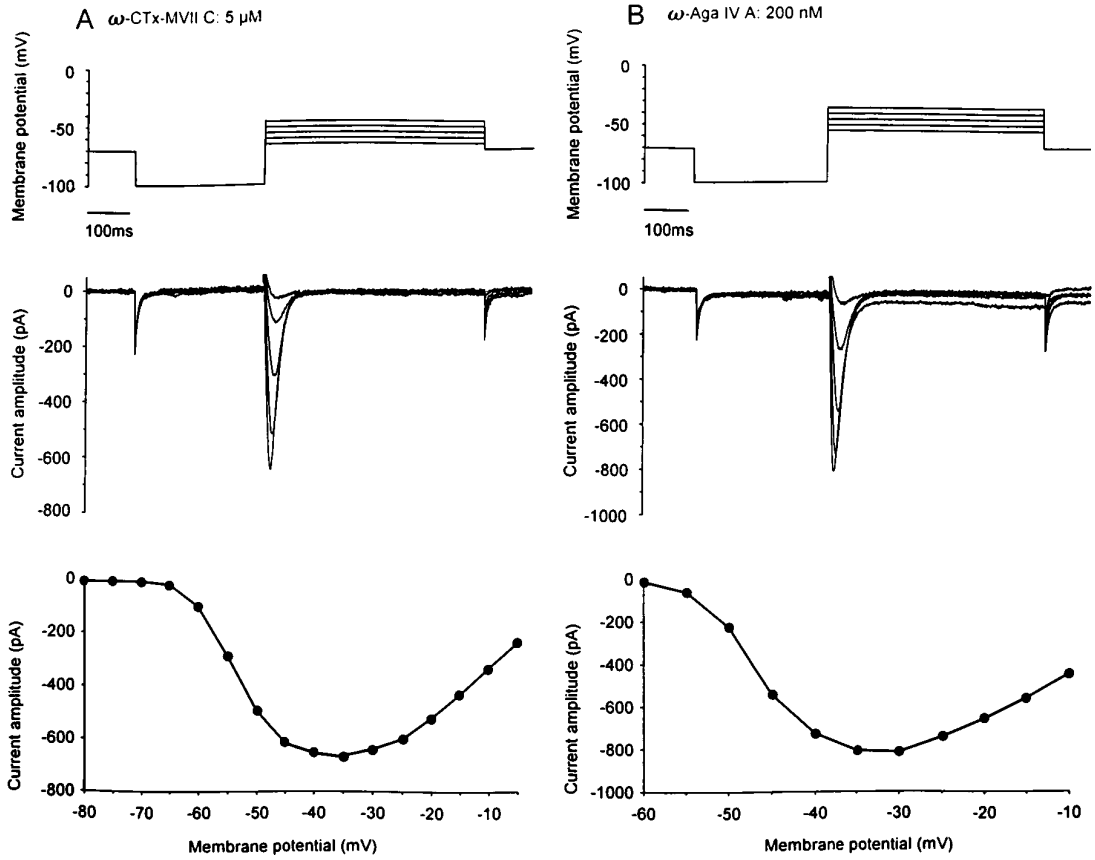

Figure 3. Isolation of a fast-inactivating Ca^{2+} current after pharmacological blockade of the slowly decaying and sustained components of the total Ca^{2+} current. *A*, The cerebellar slice culture was exposed for 30 min to a saline solution containing 5 μM ω-conotoxin-MVIIC. A series of depolarizing voltage steps (5 mV increments), applied after hyperpolarizing prepulses to −100 mV, induced a transient Ca^{2+} current that fully inactivated within the first 100 msec of the voltage jump. *B*, The slice culture was incubated for 30 min with saline containing 200 nM ω-Aga-IVA. Under these conditions, depolarizing voltage steps produced transient Ca^{2+} currents similar to those depicted in *A*.

as the difference of amplitude between the peak and the sustained currents (Fig. 2). Its amplitude remained relatively stable during at least an additional 30 min period of time (data not shown). This fast-inactivating Ca^{2+} current displayed a threshold for activation of −59 ± 2 mV and reached a maximal amplitude of −0.76 ± 0.14 nA at a membrane potential of −33 ± 2.7 mV (n = 9).

Isolation of the fast-inactivating component with toxins against the P/Q-type Ca^{2+} currents

In the presence of ATP and GTP in the pipette solution, bath-application of ω-Aga-IVA (200 nM, n = 5), a selective blocker of P/Q-type Ca^{2+} channels, reduced the amplitude of the peak current (60 ± 12%) and almost abolished the sustained component of the Ca^{2+} current (85 ± 10%), thereby unmasking a component that inactivated during the first 100 msec of the depolarizing voltage step (n = 5). Similarly, treatment of cerebellar slice cultures for 30 min with ω-conotoxin-MVIIC (5 μM, n = 5), another peptide that blocks P/Q-type Ca^{2+} channels (Hillyard et al., 1992), or with ω-Aga-IVA (200 nM) allowed isolation of the fast-inactivating Ca^{2+} current (Fig. 3, *A* and *B*, respectively). Its threshold for activation was −62 ± 0.8 mV, and the maximal amplitude was 0.62 ± 0.06 nA, achieved at a membrane potential of −33 ± 1.7 mV. These values are not significantly different from those obtained after rundown of the high-threshold Ca^{2+} currents. We thus pooled together the results obtained in both conditions (n = 19). The fast-inactivating Ca^{2+} component activated at −60.3 ± 1.1 mV and displayed a maximal amplitude of −0.69 ± 0.08 nA at a membrane potential of −33 ± 1.7 mV (Fig. 4*A*).

Taken together, our results demonstrate the presence of a fast-inactivating Ca^{2+} current in PCs that could be isolated after either rundown or pharmacological block of the slowly inactivating and sustained components of the total Ca^{2+} current.

Kinetic properties of the isolated low-threshold fast-inactivating Ca^{2+} current

The kinetics of the low-threshold Ca^{2+} current were studied at potentials varying between the threshold for activation (−60 mV) and the membrane potential showing the maximum amplitude of the current (−30 mV). The activation and inactivation of the low-threshold Ca^{2+} current could be well fitted as the sum of two exponentials at every potential tested (n = 19). The activation time constant decreased progressively from 8.7 ± 0.7 msec at −60 mV to 5.8 ± 0.5 msec at −30 mV (Fig. 4*B*, *open circles*). The inactivation time constant increased progressively from 24.5 ± 3.3 msec at −60 mV to 14 ± 0.9 msec at −30 mV (Fig. 4*B*, *filled circles*).

Activation and inactivation properties of isolated low-threshold fast-inactivating Ca^{2+} current

Step depolarizations (500 msec) to potentials between −65 and −20 mV were preceded by hyperpolarizing prepulses to −100 mV

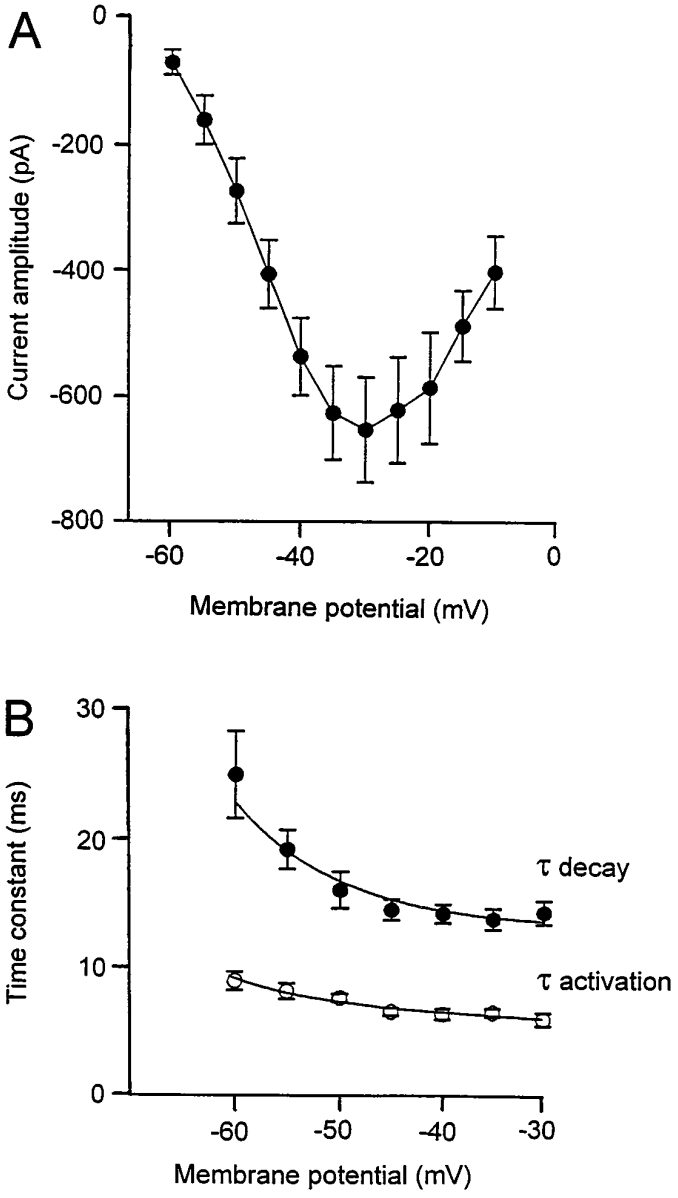

Figure 4. Characterization of the fast-inactivating Ca^{2+} current. Current–voltage relationship for the fast-inactivating Ca^{2+} current isolated either after rundown of the noninactivating components or after incubation of the slice with selective blockers of the P/Q-type Ca^{2+} channels. *B*, Time constants for activation (*open circles*) and inactivation (*filled circles*) of the transient Ca^{2+} current varied as a function of the membrane potential.

to determine the activation of the fast-inactivating Ca^{2+} current (Fig. 5*A*, *left traces*). The relative conductance as a function of the test potential could be described with a Boltzmann equation having a half-maximal conductance at −51 mV and a slope factor of 4.6 (Fig. 5*A*, *right trace*). The steady-state inactivation of the transient Ca^{2+} current was examined with step hyperpolarizing prepulses to potentials between −110 and −65 mV, followed by depolarizing voltage steps eliciting the maximal amplitude of the current (Fig. 5*B*, *left traces*). The relative amplitude of the current as a function of the hyperpolarizing prepulses was fitted with a Boltzmann equation having a half-maximal inactivation at −86 mV and a slope factor of 4.9 (Fig. 5*B*, *right trace*). The two Boltzmann functions did not overlap, indicating that the low-threshold Ca^{2+} current was not tonically activated at the resting membrane potential.

The kinetic properties of the low-threshold Ca^{2+} current described above thus closely resemble those reported for T-type Ca^{2+} currents in other cell types (Bean, 1989).

Pharmacology of the low-threshold Ca^{2+} current

The low-threshold Ca^{2+} current in PCs was further characterized pharmacologically, after blocking P/Q-type Ca^{2+} currents by incubating the cultures for 30 min in saline containing 200 nM ω-Aga-IVA. Inactivation of the low-threshold Ca^{2+} current was removed with hyperpolarizing prepulses to −100 mV (300–500 msec). Bath application of 10 μM Cd^{2+} reduced the current by 90 ± 2% (n = 5), demonstrating that it was mediated by Ca^{2+} channels. Four different compounds reported to reduce T-type Ca^{2+} currents were tested. The inorganic cation Ni^{2+} ($NiCl_2$, 100 μM; n = 5) reduced the amplitude of the current by 19 ± 2.7% (Fig. 6*A*). Amiloride (250 μM, n = 5) was the most effective drug tested, reversibly decreasing the amplitude of the low-threshold Ca^{2+} current by 53 ± 4% (Fig. 6*B*). Nifedipine (10 μM, n = 5) and baclofen (100 μM, n = 5) only weakly affected the amplitude of the fast-inactivating Ca^{2+} current (5.5 ± 1.3% and 4.6 ± 2%, respectively) (Fig. 6*C*). These pharmacological characteristics are consistent with the identification of the low-threshold fast-inactivating Ca^{2+} current present in PCs as a T-type Ca^{2+} current.

Characteristics of the Ca^{2+} channels

The cell-attached configuration of the patch-clamp technique was used to localize the channels underlying the macroscopic T-type Ca^{2+} current. Recordings were performed from either somata or dendrites of PCs, using Ca^{2+} (10 mM) as the charge carrier. The dendritic recordings were carried out from proximal primary dendrites (distance from the cell bodies, 20–50 μm) or from more distal secondary dendritic branches (distance from the cell bodies, 100–200 μm). A high density of Ca^{2+} channels producing ensemble averages with a low threshold of activation and fast inactivation were seen in 70% of dendritic recordings (n = 10). In those experiments, depolarizing voltage steps from −20 mV relative to the RP to +40 mV relative to RP elicited inward ensemble currents that completely inactivated during the first 100 msec of the depolarizing voltage step (Fig. 7*A*, *left panel*). The decay of 30 averaged current traces could be fitted with a single exponential, having a time constant of 25 ± 6 msec (n = 6). The amplitude of the inward ensemble current was plotted as a function of the pipette potential (Fig. 7*A*, *right panel*). The fast-inactivating ensemble current had a threshold for activation of +10 mV relative to RP and reached a maximal amplitude of −7.9 ± 2.1 pA (n = 6).

Similar channel activity has also been observed with somatic recordings but in only 25% of the cells tested (n = 20, not illustrated). The maximal amplitude of the transient inward ensemble current (−1.1 ± 0.9 pA) was smaller than at dendritic sites, suggesting a lower density of channels on somatic membranes. By plotting the amplitude of individual single-channel currents as a function of the pipette potential, a mean conductance of 7 ± 1 pS was determined for the somatic and dendritic channels (n = 5). In another set of experiments, the pharmacology of the ensemble currents in somatic and dendritic recordings was tested with the P/Q-type Ca^{2+} channel blocker ω-Aga-IVA. When ω-Aga-IVA (200 nM) was added to both the pipette and the extracellular solutions, depolarizing voltage steps from −20 to +30 mV (500 msec) relative to RP evoked channel activity whose

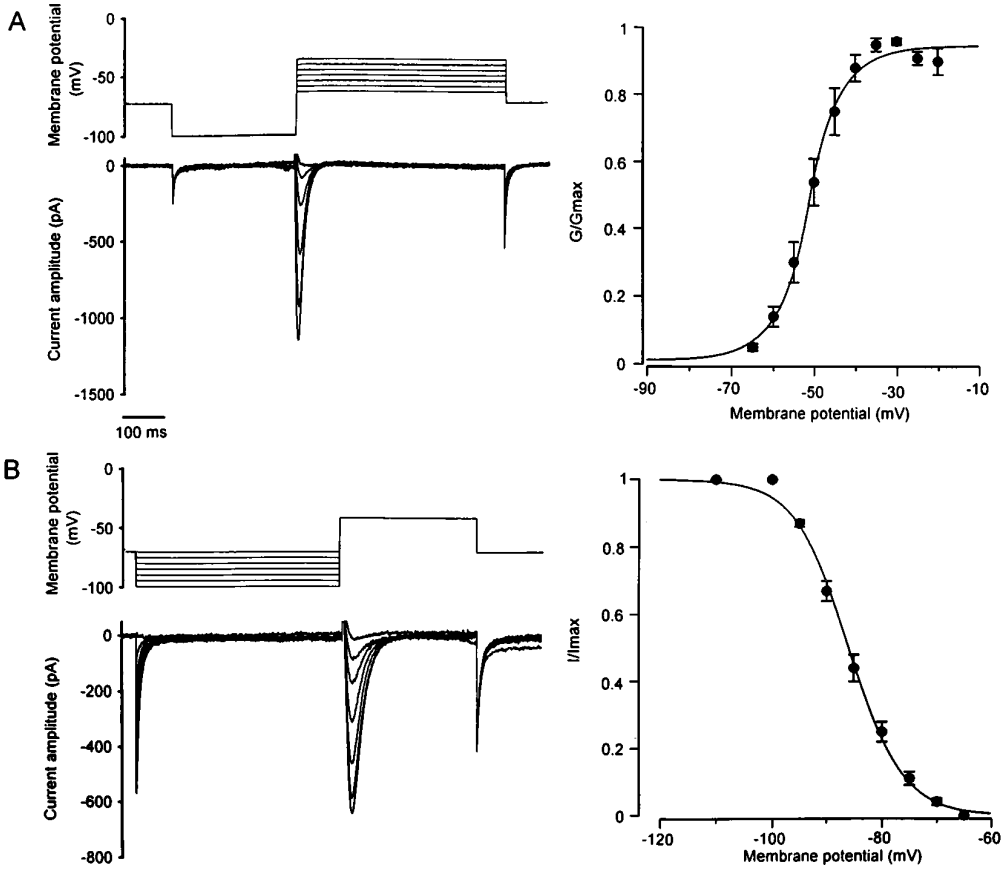

Figure 5. Activation and inactivation of the fast-inactivating Ca^{2+} current. *A*, Activation of the transient Ca^{2+} current. To remove inactivation of the current, a prepulse to −100 mV (300 msec) was applied before depolarizing voltage increments (500 msec). Representative current traces are illustrated on the *left*. The normalized conductances are described as a function of the membrane potential (*right*) and could be fitted with a Boltzmann equation, with half-maximal activation at −51 mV (n = 20). *B*, Steady-state inactivation of the fast-inactivating Ca^{2+} current. A test potential (300 msec) giving rise to the maximal current amplitude was preceded by hyperpolarizing pulses (500 msec) ranging from −110 to −65 mV. Representative current traces are illustrated on the *left*. The normalized amplitude of the current is expressed as a function of the membrane potential and described with a Boltzmann equation, with half-maximal inactivation at −86 mV (n = 20).

ensemble averages completely inactivated during the pulse in all cells tested (Fig. 7*B*, *left panel*). The threshold for activation and the maximal amplitude of the ensemble current were similar to the values obtained in control conditions (Fig. 7*B*). These results demonstrate that the P/Q-type Ca^{2+} channels contribute relatively little current in such cell-attached recordings. Taken together with the activation threshold and inactivation kinetics, we suggest rather that T-type Ca^{2+} channels underlie the bulk of the current under the present, relatively physiological, conditions.

No detectable channel activity resulting in a high-threshold sustained ensemble current was apparent in any of the dendritic or somatic membrane patches. In some dendritic recordings, however, current traces with a high level of noise, in addition to the transient inward ensemble current, were observed when the patch was depolarized to +50 mV relative to RP (data not shown). Because high-threshold Ca^{2+} channels have a greater permeability for Ba^{2+} than for Ca^{2+} (Hagiwara and Byerly, 1981), we replaced 10 mM $CaCl_2$ with 10 mM $BaCl_2$ in the pipette solution. Under these conditions, voltage steps (500 msec) from −20 mV relative to RP to test potentials ranging from +10 to +80 mV relative to RP elicited channel openings in all dendritic recordings (Fig. 8). This activity consisted of the very brief opening of many channels and gave rise to ensemble averages with both transient and sustained components. The maximal amplitude of these components was −28.5 ± 9.5 pA and −12.4 ± 2.4 pA, respectively, for a depolarization of +50 mV relative to RP (n = 8).

Such sustained channel activity was not recorded in the presence of ω-Aga-IVA (200 nM, n = 3) added to both the pipette and extracellular solutions, suggesting that P/Q-type channels underlie the high-threshold sustained ensemble Ba^{2+} current (data not shown). High-threshold channel openings could be also detected on the somatic membrane of PCs but in only 19% of the cells tested (n = 32). In three of these six cells, the channel activity was sufficient to give rise to a sustained ensemble current with a maximal amplitude of −11 ± 6 pA, for a membrane potential of +50 mV relative to RP (data not shown).

DISCUSSION

PCs in cerebellar slice cultures display a fast-inactivating Ca^{2+} current that can be recorded in isolation after either rundown or pharmacological blockade of the sustained components of the macroscopic Ca^{2+} current. Several lines of evidence indicate that the fast-inactivating Ca^{2+} current is a T-type Ca^{2+} current.

First, the threshold for activation of the transient current was −60 ± 1.1 mV, close to the value reported for T-type Ca^{2+} currents (Bean, 1989). The decay time constant (14 ± 0.9 msec at −30 mV) and half-maximal activation and inactivation (−51 and −86 mV, respectively) are similar to those of T-type Ca^{2+} currents in sensory neurons (Carbone and Lux, 1984; Bossu et al., 1985; Fox et al., 1987a), mammalian thalamic neurons (Coulter et al., 1989; Huguenard and Prince, 1992), and hippocampal pyramidal cells (O'Dell and Alger, 1991; Thompson and Wong, 1991). Second, its amplitude was affected neither by the rundown process (Bossu et al., 1985; Fedulova et al., 1985) nor by application of nifedipine, as reported for sensory neurons (Boll and Lux, 1985; Fox et al., 1987a). The transient Ca^{2+} current, however, was reduced by amiloride, a selective blocker of T-type Ca^{2+} channels (Tang et al., 1988), and to a lesser extent by Ni^{2+}, as originally reported by Carbone et al. (1987). The weak effect of Ni^{2+} (100

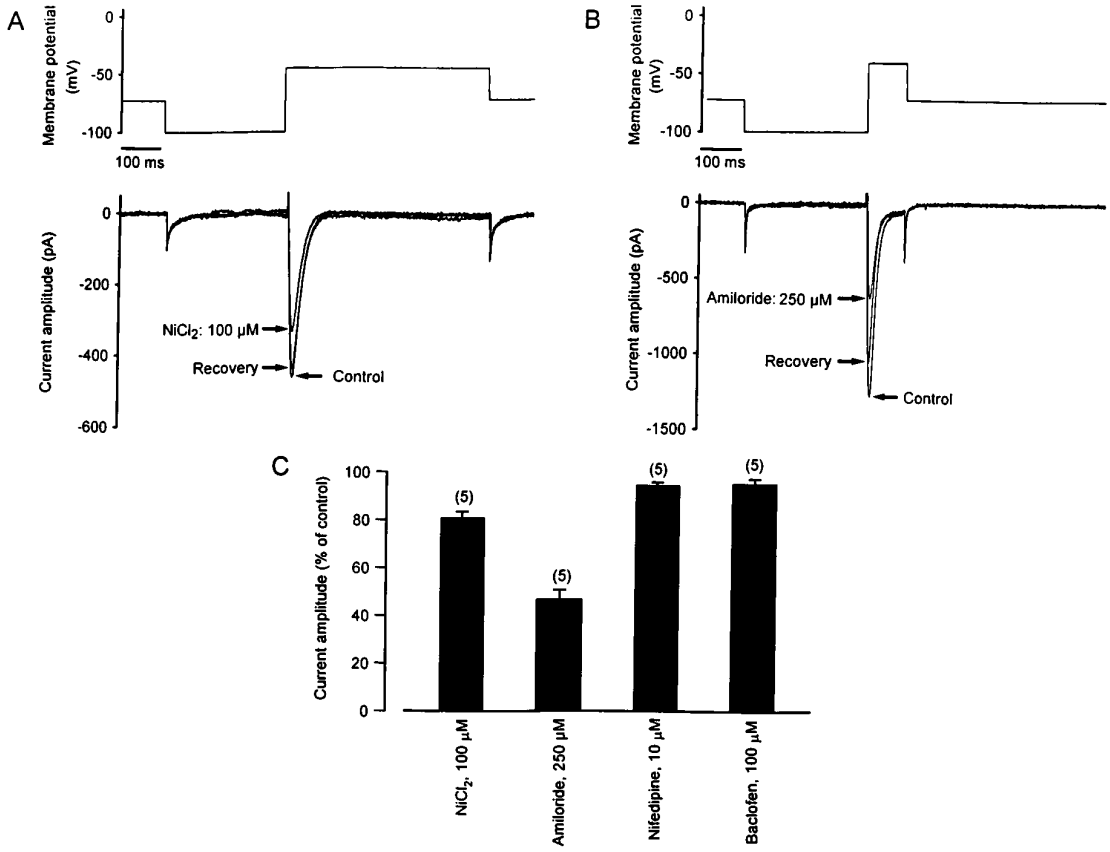

Figure 6. Pharmacology of the fast-inactivating Ca^{2+} current. *A*, Bath application of $NiCl_2$ (100 μM) reversibly reduced the transient Ca^{2+} current amplitude by 20%. *B*, The amplitude of the fast-inactivating Ca^{2+} current was also reversibly diminished (50%) with bath application of amiloride (250 μM). *C*, Summary of the pharmacology of the fast-inactivating Ca^{2+} current. The amplitude of the current in control condition was normalized to 100%. Note that only amiloride and $NiCl_2$ significantly decreased the amplitude of the transient Ca^{2+} current, whereas baclofen and nifedipine had only minor effects.

μM) may reflect a particular property of LVA Ca^{2+} currents in PCs in cerebellar slice cultures, because Ni^{2+} (25–100 μM) strongly reduced LVA Ca^{2+} current in embryonic hippocampal neurons (Ozawa et al., 1989) and DRG neurons (Fox et al., 1987a) as well as various thalamic cells (Coulter et al., 1989; Huguenard and Prince, 1992). On the other hand, higher concentrations (200–600 μM) were needed in other neuronal cells (Akaike et al., 1989; Crunelli et al., 1989; Barish, 1991).

The data obtained with the cell-attached recording configuration with Ca^{2+} as the charge carrier revealed the existence of a voltage-activated channel activity that gave rise to a transient ensemble Ca^{2+} current that was insensitive to ω-Aga-IVA. The threshold for activation of the transient ensemble Ca^{2+} current was 0 to +10 mV relative to RP, a value that is compatible with the threshold of the T-type Ca^{2+} current (−60 ± 1.1 mV), given that the RP of PCs ranges between −70 and −60 mV in sharp electrode recordings (D. Mouginot, unpublished observations). In addition, the transient ensemble current displayed fast inactivation kinetics with a time constant of 25 ± 6 msec, comparable to the time constant of 24.6 ± 2 msec for the fast component of the macroscopic Ca^{2+} current. Finally, the conductance of the Ca^{2+} channels in PCs was 7 ± 1 pS, a value that is similar to that of T-type Ca^{2+} channels in primary cultures of dissociated PCs (Bossu et al., 1989b), sensory neurons (Carbone and Lux, 1984; Nowycky et al., 1985), and hippocampal neurons (Fisher et al., 1990; O'Dell and Alger, 1991), when Ba^{2+} (110 mM) was used as the charge carrier.

Our data indicate that the sustained Ca^{2+} current is a member of the P/Q-type Ca^{2+} current family. First, the sustained Ca^{2+} current had a threshold for activation of −43 ± 1 mV and showed weak inactivation during depolarizing voltage steps, a property that characterizes these Ca^{2+} currents (Bean, 1989; Zhang et al., 1993). Maximal current amplitudes were reached at approximately −30 mV, which supports the view that high-threshold Ca^{2+} currents in PCs peak at more negative potentials than they do in most other neurons (Regan et al., 1991). In the absence of ATP and GTP in the pipette solution, the sustained Ca^{2+} current underwent a time-dependent reduction of its amplitude, as observed consistently during WCRs of high-threshold currents (Bossu et al., 1985; Fedulova et al., 1985). Second, the sustained Ca^{2+} current described in this study was reduced markedly by ω-Aga-IVA and by ω-conotoxin-MVIIC, two potent inhibitors of the P/Q-type Ca^{2+} current (Hillyard et al., 1992; Mintz et al., 1992a,b). Third, sustained channel activity was detected readily in cell-attached recordings in which Ba^{2+} was used as the charge carrier. This channel activity presumably underlies the sustained Ca^{2+} current seen in macroscopic recordings, because it was not apparent when ω-Aga-IVA was present in both the pipette and the extracellular solutions. The sustained channel activity could not be resolved sufficiently when the charge was carried by Ca^{2+},

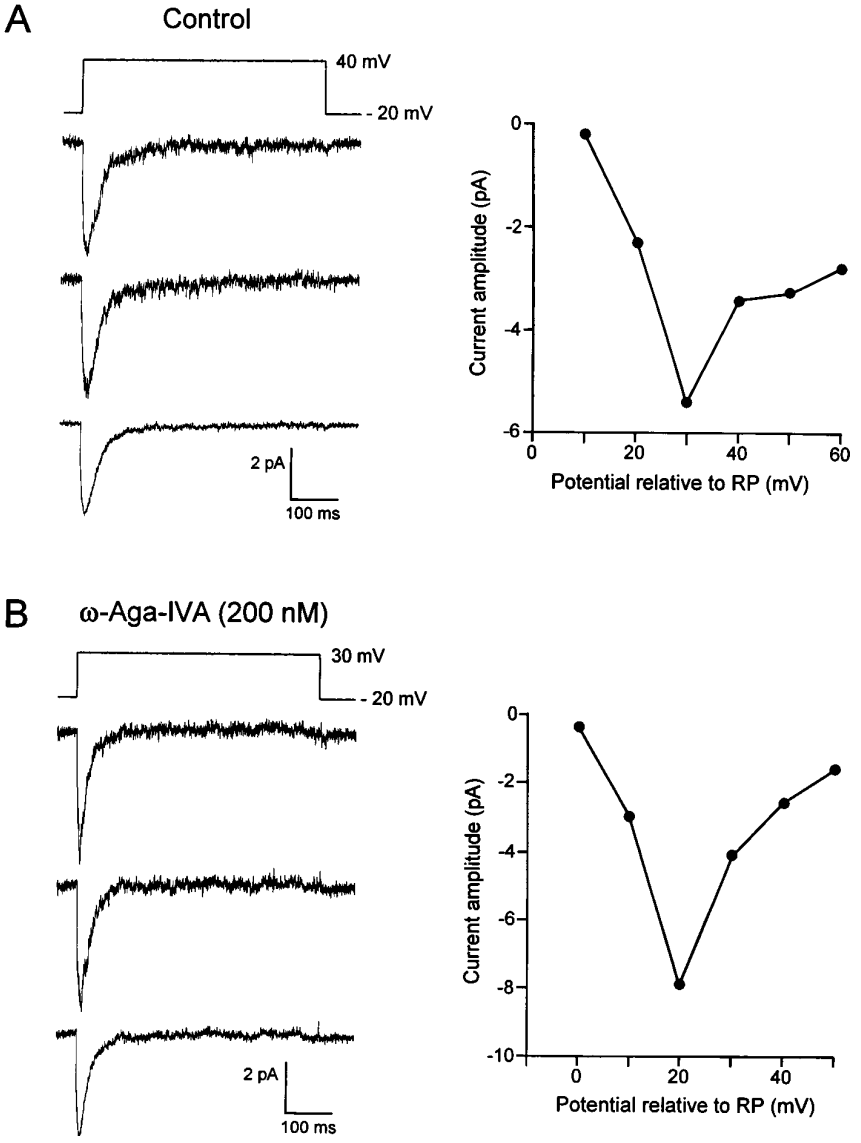

Figure 7. Ca^{2+} channel activity recorded from dendrites of PCs using Ca^{2+} as the charge carrier. *A*, Example of Ca^{2+} channel activity recorded under control conditions. The patch membrane was depolarized from −20 mV to +40 mV relative to RP. The *two top traces* represent single current traces, whereas the *third trace* illustrates the ensemble current obtained from 30 averaged individual current traces. The *right panel* shows the current–voltage relationship obtained in the same cell. *B*, Example of Ca^{2+} channel activity recorded with ω-Aga-IVA (200 nM) in both the pipette and extracellular solutions. The patch membrane was depolarized from −20 to +30 mV relative to RP. The *two top traces* illustrate individual current traces, whereas the *third trace* represents the ensemble current obtained from 30 averaged individual current traces. The *right panel* shows the current–voltage relationship of the ensemble current measured at the peak of the response.

indicating that the conductance of the P/Q-type channels is greater for Ba^{2+} than for Ca^{2+}, as reported for P/Q-type Ca^{2+} channels isolated from squid optic lobe and incorporated into artificial lipid membranes (Llinás et al., 1989). In addition, these Ca^{2+} channels may be highly sensitive to Ca^{2+}-dependent inactivation induced by Ca^{2+} influx through these channels.

The cell-attached configuration of the patch-clamp technique allowed the localization of the channels underlying both T-type and P/Q-type Ca^{2+} currents in PCs. T-type Ca^{2+} channel activity was recorded from both dendrites and somata of PCs. T-type channel activity was uncommon (25% of the cells tested) in somatic recordings, however, and the amplitude of the transient ensemble Ca^{2+} current in these patches was smaller than in dendritic patches. A dendritic localization of T-type Ca^{2+} currents has been reported for PCs in dissociated cultures derived from young rats (Bossu et al., 1989b), in acutely dissociated hippocampal neurons (O'Dell and Alger, 1991), and in CA1 pyramidal cells in hippocampal slices (Karst and Wadman, 1993). In contrast, a somatic location of T-type Ca^{2+} channels was suggested by data obtained with intracellular recordings from inferior olive neurons (Llinás and Yarom, 1981), as well as by single-channel recordings from acutely isolated cell bodies of thalamic neurons (Suzuki and Rogawski, 1989), from sensory neurons (Fox et al., 1987b), and from somata of CA3 pyramidal cells (Fisher et al., 1990). These studies, however, do not exclude the presence of T-type Ca^{2+} channels on dendritic membranes.

In cerebellar slice cultures, P/Q-type Ca^{2+} channel activity was detected mainly on dendritic membranes of PCs. These results are in agreement with a previous single-channel study carried out on acute cerebellar slices from guinea pigs (Usowicz et al., 1992), as well as with immunohistochemical data obtained from rat cerebellar PCs (Hillman et al., 1991). Similarly, the K^+-induced increase in the intradendritic free Ca^{2+} concentration in cultured rat cerebellar PCs was blocked by ω-Aga-IVA (Bindokas et al., 1993). Although only 19% of somatic patches displayed high-threshold channel activity in cerebellar slice cultures, the amplitude of the sustained ensemble current, when present, was comparable in somatic and dendritic locations. These results therefore support the hypothesis that P/Q-type Ca^{2+} channels are present in high densities at hot spots of somatic membranes, as also sug-

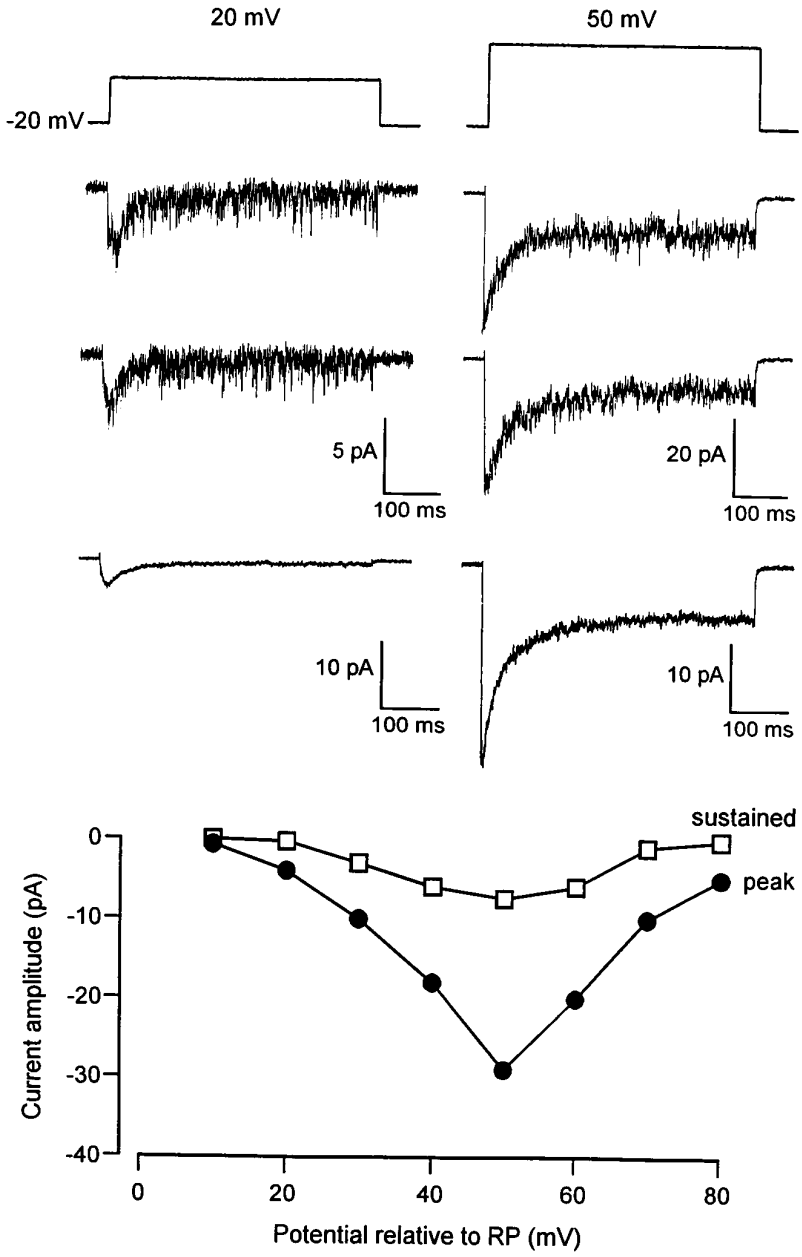

Figure 8. Dendritic channel activity recorded with Ba^{2+} as the charge carrier. The patch membrane was depolarized from −20 mV to +20 mV (*left*) and to +50 mV (*right*) relative to RP. The *two top traces* in each column represent individual current traces, and the *third trace* illustrates the ensemble current obtained from 30 averaged individual traces. A sustained ensemble current was clearly resolved under these experimental conditions, and the *bottom panel* depicts the current–voltage relationship for both the peak (*filled circles*) and the sustained (*open squares*) ensemble current.

gested by recent Ca^{2+} imaging data from somatic membranes of PCs (Kano et al., 1995).

Although there is general agreement about the existence of P/Q-type Ca^{2+} channels in cerebellar PCs, there is no consensus with respect to the presence of T-type Ca^{2+} channels. Macroscopic T-type Ca^{2+} currents have been identified in cultures of dissociated PCs derived from embryonic rat pups (Hirano and Hagiwara, 1989), in young and adult rats (Kaneka et al., 1990; Regan, 1991), and in cultured PCs from newborn rats (Bossu et al., 1989a,b). Furthermore, a recent single-channel study on rat cerebellar slices reported the presence of multiple types of Ca^{2+} channels on somata and dendrites of PCs. One of these channels activates at low threshold and shows marked inactivation. Although not pharmacologically identified, this channel may thus represent T-type Ca^{2+} channels of young adult rat PCs (Dupere and Usowicz, 1996).

On the other hand, other researchers working with dissociated PCs from young rats (Mintz et al., 1992a,b) or with acute cerebellar slices of adult guinea pigs (Usowicz et al., 1992) failed to find a low-threshold-activated Ca^{2+} current. One possible explanation for these seemingly contradictory data is that T-type Ca^{2+} channels may be more prominent in immature neurons, as shown for embryonic spinal cord neurons of *Xenopus* (Barish, 1991) and cultures of embryonic hippocampal (Meyers and Barker, 1989; O'Dell and Alger, 1991) and sensory neurons (Gottmann et al., 1988). The density of the T-type Ca^{2+} channels decreases with development in hippocampal pyramidal cells (Thompson and Wong, 1991; but see Karst and Wadman, 1993), in *Xenopus* spinal neurons (Gu and Spitzer, 1993), and in chick motoneurons (McCobb et al., 1989). The failure to detect T-type Ca^{2+} currents also may be attributable to the fact that these channels were partially inactivated. In-

deed, PCs were often held at membrane potentials of −70 to −80 mV (Llano et al., 1994; Kano et al., 1995), and our data showed that half-maximal inactivation occurs at −86 mV. In other studies, T-type Ca^{2+} currents may not have been recorded, because PCs in these preparations lacked extended dendrites (e.g., Mintz et al., 1992b).

It will be of interest to determine the physiological implications of Ca^{2+} entry through low-threshold Ca^{2+} channels in PCs. It should be noted that our results were obtained from relatively young tissue (2–4 weeks *in vitro*, derived from neonatal rat pups), and therefore these properties may not reflect the physiology of mature PCs. Preliminary evidence indicates that these Ca^{2+} channels do not play a role in synaptic transmission between PCs and deep nuclei neurons in cerebellar slice cultures. Indeed, intracellular recordings from deep cerebellar nuclear neurons indicated that synaptic potentials induced by stimulation of PCs are fully blocked by antagonists of the P/Q-type Ca^{2+} channels (D. Mouginot, unpublished observations). Similar conclusions were drawn from studies with acute cerebellar slices in which IPSCs were abolished almost completely with P- and N-type Ca^{2+} channel antagonists (Takahashi and Momiyama, 1993). The preferential localization of T channels on dendrites, however, suggests a role in synaptic integration, for example, by producing Ca^{2+} oscillations that could modulate glutamate receptor function. Because T-type channels may be expressed preferentially in immature PCs, they may be implicated in the development of autorhythmic behavior necessary for the generation of synaptic connections (Llinás, 1987).

REFERENCES

Akaide N, Kostyuk PG, Osipchuk YV (1989) Dihydropyridine-sensitive low-threshold calcium channels in isolated rat hypothalamic neurones. J Physiol (Lond) 412:181–195.

Barish ME (1991) Voltage-gated calcium currents in cultured embryonic *Xenopus* spinal neurones. J Physiol (Lond) 444:523–543.

Bean BP (1989) Classes of calcium channels in vertebrate cells. Annu Rev Physiol 51:367–384.

Bindokas VP, Brorson JR, Miller RJ (1993) Characteristics of voltage sensitive calcium channels in dendrites of cultured rat cerebellar neurons. Neuropharmacology 32:1213–1220.

Boll W, Lux HD (1985) Action of organic antagonists on neuronal calcium currents. Neurosci Lett 56:335–339.

Bossu J-L, Feltz A, Thomann JM (1985) Depolarization elicits two distinct calcium currents in vertebrate sensory neurones. Pflügers Arch 403:360–368.

Bossu J-L, Dupont J-L, Feltz A (1989a) Calcium currents in rat cerebellar Purkinje cells maintained in culture. Neuroscience 30:605–617.

Bossu J-L, Fagni L, Feltz A (1989b) Voltage-activated calcium channels in rat Purkinje cells maintained in culture. Pflügers Arch 414:92–94.

Bossu J-L, De Waard M, Feltz A (1991) Two types of calcium channels are expressed in adult bovine chromaffin cells. J Physiol (Lond) 437:621–634.

Carbone E, Lux HD (1984) A low voltage-activated, fully inactivating Ca^{2+} channel in vertebrate sensory neurones. Nature 310:501–502.

Carbone E, Morad M, Lux HD (1987) External Ni^{2+} selectively blocks the low-threshold Ca^{2+} current of chick sensory neurons. Pflügers Arch 408:R60.

Coulter DA, Huguenard JR, Prince DA (1989) Calcium currents in rat thalamocortical relay neurones: kinetic properties of the transient low-threshold current. J Physiol (Lond) 414:587–604.

Crunelli V, Lightowler S, Pollard CE (1989) A T-type Ca^{2+} current underlies low-threshold Ca^{2+} potentials in cells of the cat and rat lateral geniculate nucleus. J Physiol (Lond) 413:543–561.

Dupere JRB, Usowicz MM (1996) Multiple types of Ca^{2+} channels in the soma and dendrites of adult rat cerebellar Purkinje cells. J Physiol (Lond), in press.

Fedulova SA, Kostyuk P, Veselovsky NY (1985) Two types of calcium channels in the somatic membrane of newborn rat dorsal root ganglion neurones. J Physiol (Lond) 359:431–446.

Fisher RP, Gray R, Johnson D (1990) Properties and distribution of single voltage-gated calcium channels in adult hippocampal neurons. J Neurophysiol 64:91–104.

Fox AP, Nowycky MC, Tsien RW (1987a) Kinetic and pharmacological properties distinguishing three types of Ca^{2+} currents in chick sensory neurones. J Physiol (Lond) 394:149–172.

Fox AP, Nowycky MC, Tsien RW (1987b) Single channel recordings of three types of calcium channels in chick sensory neurones. J Physiol (Lond) 394:173–200.

Gähwiler BH (1981) Organotypic monolayer cultures of nervous tissue. J Neurosci Methods 4:329–342.

Gottmann K, Dietzel ID, Lux HD, Huck S, Rohrer H (1988) Development of inward currents in chick sensory and autonomic neuronal precursor cells in culture. J Neurosci 8:3722–3732.

Gu X, Spitzer NC (1993) Low-threshold Ca^{2+} current and its role in spontaneous elevations of intracellular Ca^{2+} in developing *Xenopus* neurons. J Neurosci 13:4936–4948.

Hagiwara S, Byerly L (1981) Calcium channel. Annu Rev Neurosci 4:69–125.

Hillman D, Chen S, Aung TT, Cherksey B, Sugimori M, Llinás R (1991) Localization of P-type calcium channels in the central nervous system. Proc Natl Acad Sci USA 88:7076–7080.

Hillyard DR, Monje VD, Mintz IM, Bean BP, Nadasdi L, Ramachandran J, Miljanich G, Azimi-Zoonooz A, McIntosh JM, Cruz LJ, Imperial JS, Olivera BM (1992) A new conus peptide ligand for mammalian presynaptic calcium channels. Neuron 9:69–77.

Hirano T, Hagiwara S (1989) Kinetics and distribution of voltage-gated Ca, Na and K channels on the somata of rat cerebellar Purkinje cells. Pflügers Arch 413:463–469.

Huguenard JR, Prince DA (1992) A novel T-type current underlies prolonged Ca^{2+} -dependent burst firing in GABAergic neurons of rat thalamic reticular nucleus. J Neurosci 12:3804–3817.

Kaneka M, Wakamori M, Ito C, Akaike N (1990) Low-threshold calcium current in isolated Purkinje cell bodies of rat cerebellum. J Neurophysiol 63:1046–1051.

Kano M, Schneggenburger R, Verkhratsky A, Konnerth A (1995) Depolarization-induced calcium signals in the somata of cerebellar Purkinje neurons. Neurosci Res 24:87–95.

Karst H, Wadman WJ (1993) Low-threshold calcium current in dendrites of the adult rat hippocampus. Neurosci Lett 164:154–158.

Llano I, DiPolo R, Marty A (1994) Calcium-induced calcium release in cerebellar Purkinje cells. Neuron 12:663–673.

Llinás R (1987) "Mindness" as a functional state of the brain. In: Mindwaves. Thoughts on intelligence, identity and consciousness (Blakemore C, Greenfield S, eds). Oxford: Basil Blackwell.

Llinás R, Sugimori M (1980a) Electrophysiological properties of in vitro Purkinje cell dendrites in mammalian cerebellar slices. J Physiol (Lond) 305:197–213.

Llinás R, Sugimori M (1980b) Electrophysiological properties of in vitro Purkinje cell somata in mammalian cerebellar slices. J Physiol (Lond) 305:171–195.

Llinás R, Yarom Y (1981) Properties and distribution of ionic conductances generating electroresponsiveness of olivary neurones in vitro. J Physiol (Lond) 315:569–584.

Llinás R, Sugimori M, Lin J-W, Cherksey B (1989) Blocking and isolation of a calcium channel from neurons in mammals and cephalopods utilizing a toxin fraction (FTX) from funnel-web spider poison. Proc Natl Acad Sci USA 86:1689–1693.

McCleskey EW (1994) Calcium channels: cellular roles and molecular mechanisms. Curr Opin Neurobiol 4:304–312.

McCobb DP, Best PM, Beam KG (1989) Development alters the expression of Ca^{2+} currents in chick limb motoneurons. Neuron 2:1633–1643.

Meyers DE, Barker JL (1989) Whole-cell patch-clamp analysis of voltage-dependent calcium conductances in cultured embryonic rat hippocampal neurons. J Neurophysiol 61:467–477.

Mintz IM, Adams ME, Bean BP (1992a) P-type calcium channels in rat central and peripheral neurons. Neuron 9:85–95.

Mintz IM, Venema VJ, Swiderek KM, Lee TD, Bean BP, Adams ME (1992b) P-type calcium channels blocked by the spider toxin omega-Aga-IVA. Nature 355:827–829.

Nowycky MC, Fox AP, Tsien RW (1985) Three types of neuronal calcium channels with different calcium agonist sensitivity. Nature 316:440–443.

O'Dell TJ, Alger BE (1991) Single channels in rat and guinea-pig hippocampal neurons. J Physiol (Lond) 436:739–767.

Ozawa S, Tsuzuki K, Iino M, Ogura A, Kudo Y (1989) Three types of voltage-dependent calcium currents in cultured rat hippocampal neurons. Brain Res 495:329–336.

Regan LJ (1991) Voltage-dependent calcium currents in Purkinje cells from rat cerebellar vermis. J Neurosci 11:2259–2269.

Regan LJ, Sah DWY, Bean BP (1991) Calcium channels in rat central and peripheral neurons: high threshold current resistant to dihydropyridine blockers and ω-conotoxin. Neuron 6:269–280.

Snutch TP, Reiner PB (1992) Ca^{2+} channels: diversity of form and function. Curr Opin Neurobiol 2:247–253.

Stea A, Tonlinson WJ, Soong TW, Bourinet E, Dubel SJ, Vincent SR, Snutch TP (1995) Localization and functional properties of a rat brain alpha 1A calcium channel reflect similarities to neuronal Q and P-type Ca^{2+} channels. Proc Natl Acad Sci USA 91:10576–10580.

Suzuki S, Rogawski MA (1989) T-type calcium channels mediate the transition between tonic and phasic firing in thalamic neurons. Proc Natl Acad Sci USA 86:7228–7232.

Takahashi T, Momiyama M (1993) Different types of calcium channels mediate central synaptic transmission. Nature 366:156–158.

Tang CM, Presser F, Morad M (1988) Amiloride selectively blocks the low threshold (T) calcium channel. Science 240:213–215.

Thompson SM, Wong RKS (1991) Development of calcium current subtypes in isolated rat hippocampal pyramidal cells. J Physiol (Lond) 439:671–689.

Tsien RW, Ellinor PT, Horne WA (1991) Molecular diversity of voltage-dependent Ca^{2+} channels. Trends Pharmacol Sci 12:349–354.

Usowicz MM, Sugimori M, Cherksey B, Llinás R (1992) P-type calcium channels in the somata and dendrites of adult cerebellar Purkinje cells. Neuron 9:1185–1199.

Zhang JF, Randall A, Ellinor PT, Horne W, Sather WA, Tanabe T, Schwartz TL, Tsien RW (1993) Distinctive pharmacology and kinetics of cloned neuronal Ca^{2+} channels and their possible counterparts in mammalian CNS neurons. Neuropharmacology 32:1075–1088.